Available online at www.sciencedirect.com
SCIENCE DIRECT®
Journal of Catalysis 223 (2004) 212–220
JOURNAL OF CATALYSIS
www.elsevier.com/locate/jcat

Kinetic study of photocatalytic oxidation of adsorbed carboxylic acids at TiO_2 porous films by photoelectrolysis

Dianlu Jiang, Huijun Zhao,* Shanqing Zhang, and Richard John

School of Environmental and Applied Sciences, Gold Coast Campus, Griffith University, PMB 50, Gold Coast Mail Center, Queensland 9726, Australia

Received 12 September 2003; revised 28 January 2004; accepted 29 January 2004

Abstract

A unique transient photoelectrolysis technique was developed to study the photocatalytic oxidation kinetics of adsorbed organic compounds at particulate TiO_2 film electrodes. The technique was employed to study the photocatalytic oxidation of a number of adsorbed dicarboxylic acids at TiO_2 porous film electrodes. The adsorption of these compounds was found to be heterogeneous, with three major types of surface complexes identified—each having distinctive binding affinities to the TiO_2 surface. The three thermodynamically distinctive types of surface complexes exhibit two measurable photocatalytic reaction kinetic characteristics, i.e., a fast process and a slow process. The fast kinetic process can be attributed to the photocatalytic degradation of the strongest adsorbed species at more active sites such as edge and corner titanium ions. The slow kinetic process can be attributed to the photocatalytic degradation of the medium-strength bound complexes and the weakest bound surface complexes. The rate constants for these processes were calculated by curve fitting the photocurrent transient response to a double exponential decay expression. For adsorbed oxalic acid both the fast and the slow processes were shown to be the first-order processes in which both rate constants were independent of surface coverage. For the larger dicarboxylic acids adsorbed, the rate constant for the fast photocatalytic process (k_f) was found to decrease with an increase in the surface coverage. The rate constant for the slow photocatalytic process, however, was shown to be a true first-order process for all adsorbed dicarboxylic acids. The value of the rate constant (k_s) was similar for all the adsorbates studied and was independent of the surface coverage.

Keywords: Porous TiO_2; Photocatalysis; Photoelectrochemistry; Adsorption; Dicarboxylic acid

1. Introduction

In order to improve the photocatalytic efficiency at TiO_2 surfaces, a great deal of effort has been devoted in recent years to the study of the kinetics of photocatalytic processes [1–6]. To date, most of the kinetic studies of the photocatalytic oxidation at TiO_2 surface have been carried out using a particulate TiO_2 suspension/slurry system [2,7–14]. This approach involves complex, tedious, and time-consuming procedures and it is extremely difficult to control the experiment under desired conditions [15,16]. In addition, it is also impossible to obtain instantaneous reaction rates with such an approach. Usually the concentration change in bulk solution within a given time interval (i.e., at least a few minutes) is measured to obtain the initial reaction rate. During this period, both the concentration and the composition of the sample solution can change markedly. The concentration change is caused not only by the photocatalytic reaction of the original compounds but also by adsorption, particularly, for strong adsorbates, while the formation of intermediates can also change the composition. The case may become even more complicated when the surface reactivity of the photocatalyst is affected by the intermediates. The apparent reaction rate thus obtained is a collective result of many factors. As a result, this type of apparent reaction rate provides very limited useful information in understanding the kinetics of a photocatalytic process. This is especially true when the reactant is a strong adsorbate, where the physical meaning of the initial rate obtained cannot be clearly defined due to the loss of the reactant from the solution phase and the extra occupancy of the surface caused by adsorption [11]. Furthermore, the radiation field is usually poorly defined in too many papers on the kinetic studies in TiO_2 slurry systems, which makes the kinetic data reported by different groups incomparable.

* Corresponding author.
E-mail address: h.zhao@griffith.edu.au (H. Zhao).

0021-9517/$ – see front matter
doi:10.1016/j.jcat.2004.01.030

It has long been known that the adsorption of organic substrates onto TiO_2 photocatalysts has a great impact on the photocatalytic oxidation kinetics and often these photocatalytic processes can be represented by the Langmuir–Hinshelwood kinetic expression [4,9,13,17–21]. Despite this, lack of correlation between photocatalytic reaction rates and dark adsorption amounts has been reported [4,11–13]. In addition, inconsistencies between the adsorption equilibrium constant obtained from the Langmuir–Hinshelwood treatment of kinetic data and from the dark adsorption data have been frequently reported [4,11–13]. These contradictions cannot be explained without the proper understanding of the photohole capture kinetics of adsorbed compounds.

High photocatalytic efficiency is the ultimate goal pursued by researchers in photocatalysis. To this end, a better understanding of the photocatalytic degradation kinetics of organic compounds is crucial. In this work, we propose a new photoelectrolysis technique to study the photocatalytic oxidation kinetics of adsorbed organic compounds in aqueous media. This technique is capable of providing useful kinetic information in a direct, simple, and rapid manner. To our knowledge, this is the first time such a technique has been employed to study the kinetics of photocatalytic degradation of organic compounds in an aqueous solution.

The proposed technique utilizes a TiO_2 porous film electrode, which is fabricated by immobilization of TiO_2 particles onto a conducting substrate. This allows the use of simple electrochemical techniques to acquire data. The methodology involves a two-step measurement procedure in which an adsorption step is carried out before the photoelectrochemical measurement. This physical separation of the adsorption process from the photoelectrochemical oxidation process simplifies the system and allows a detailed study of the kinetic process of interest without the influence of bulk solution effects such as diffusion limitations. This is in contrast to kinetic studies carried out in bulk solution where diffusion of organic compounds to be oxidized can be a limiting step, and the organic compound in solution and in the adsorbed form could complicate the overall kinetic behaviour.

For a given organic compound, the surface coverage (or the amount adsorbed) at a TiO_2 porous film electrode depends on the concentration of the compound and the adsorption time. In the technique used in this study, this amount can be readily quantified in the subsequent photoelectrochemical oxidation process [15]. At a given illumination light intensity, when a suitable potential bias is applied to ensure that the overall rate of reaction is not controlled by the electron transport across the TiO_2 film or by the electron removal at the electrode/solution interface, the photocurrent obtained should reflect the photocatalytic degradation rate of the adsorbed organic compounds. Based on this concept, the photocatalytic oxidation kinetics of the adsorbed organic compounds can be directly studied.

A group of dicarboxylic acids was chosen as model compounds for this study because of their well-known adsorption properties at TiO_2 surfaces [22,23]. The simplest dicarboxylic acid, oxalic acid, was first investigated due to the fact that complete mineralization of one oxalic molecule requires only two electrons and involves the least number of intermediates. This makes its overall photocatalytic degradation process the simplest among all dicarboxylic acids. Down the series from oxalic acid to glutaric acid, the number of electrons required and the number of steps and intermediates involved for complete mineralization are increased. The adsorption behaviour and the relationship between photocatalytic oxidation kinetics and adsorption of these model compounds were investigated. Of particular interest, was how the photocatalytic kinetic behaviour changed with an increase in complexity of the adsorbate given that complete mineralization of the larger dicarboxylic acids involves an increase in number of degradative steps and reaction intermediates.

2. Experimental

2.1. Materials

Indium tin oxide-conducting glass slides (ITO, 8 Ω/square) were purchased from Delta Technologies Limited (USA). Titanium butoxide (97%, Aldrich), oxalic acid (AR, Ajax Chemicals), succinic acid (99%, Sigma), malonic acid (Sigmaultra, Sigma), glutaric acid (99%, Sigma), and carbowax 20M (Supelco) were used as received. All other chemicals were of analytical grade and purchased from Aldrich unless otherwise stated. All solutions were prepared using high-purity deionised water (Millipore Corp., 18 MΩ cm).

2.2. Preparation of the porous TiO_2 film electrode

An aqueous TiO_2 colloid was prepared by hydrolysis of titanium butoxide according to the method described by Nazeeruddin et al. [24]. The resultant colloidal solution contains ca. 60 g dm^{-3} of TiO_2 solid with particle sizes ranging from 8 to 10 nm. Carbowax (30% w/w based on the solid weight of the TiO_2 colloid) was added to increase the porosity of the final TiO_2 film. ITO slides were used as the conducting substrate and details of ITO pretreatment can be found in our previous publications [15]. After pretreatment, the ITO slides were dip-coated in the TiO_2 colloidal solution. The coated electrodes were then calcined in a muffle furnace at 500 °C for 30 min in air. The thickness of the film was about 1.0 μm measured with a surface profilometer (Alpha-step 200, Tencor Instrument). Characterised by X-ray diffraction (Philips PW1050) and scanning electron microscope (JSM-6400F, JEOL) the film was of nanoporous structure and consisted of a pure anatase phase.

2.3. Apparatus and methods

All experiments were performed at ca. 23 °C in a conventional three-electrode electrochemical cell with a quartz window for illumination. The TiO_2 film electrodes described in the previous section were employed as a working electrode. The electrode was mounted onto an electrode holder with an area of 0.65 cm^2 left unsealed to be exposed to the solution for illumination and for photoelectrochemical reaction. A saturated Ag/AgCl electrode and a platinum mesh were used as the reference and the auxiliary electrodes, respectively. To eliminate the influence of solution resistance, 0.1 M $NaNO_3$ was chosen as the supporting electrolyte. A voltammograph (CV-27, BAS) was used for application of potential bias in the phototransient experiments and linear potential sweep experiments. Potential and current signals were recorded using a Macintosh computer (7220/200) coupled to a Maclab 400 interface (AD Instruments). The illumination was carried out using a 150 W xenon arc lamp light source with focusing lenses (HF-200w-95, Beijing Optical Instruments). Light intensity was measured with a UV-irradiance meter (UVA, Instruments of Beijing Normal University), and was 6.6 mW cm^{-2} unless otherwise stated. To avoid the sample solution being heated by the infrared light, the light beam was passed through an UV-band pass filter (UG 5, Avotronics Pty. Limited).

For the measurement of transient photoelectrolysis of preadsorbed organic compounds the TiO_2 nanoporous film electrode was immersed in a given concentration adsorbate solution with 0.1 M $NaNO_3$ at pH 4.0 for 30 min to allow equilibrium to be reached. The electrode was then washed with 0.1 M $NaNO_3$ solution and immediately transferred to a photoelectrochemical cell (containing 0.1 M $NaNO_3$ solution) where photoelectrolysis was performed.

3. Results and discussion

3.1. Selection of potential bias

The applied potential bias affects the kinetics of a photoelectrolysis process by facilitating the process of electron transport across the semiconductor film [16]. In order to focus the investigation on the kinetic process of interest, an appropriate potential bias is needed. To this end, linear sweep voltammetry was performed at the TiO_2 nanoporous electrode in solutions of organic compounds. Fig. 1 shows the typical voltammograms of oxalic acid at a TiO_2 porous electrode with and without UV illumination. When the experiment was carried out without illumination (in the dark), a cathodic current was observed at lower potentials (below -0.2 V). This can be attributed to the direct electrochemical reduction of water at bare ITO sites. The close to zero current at higher potentials (above -0.2 V) indicates that the direct electrochemical reaction at bare ITO sites was not occurring (e.g., see Fig. 1, curve a). Under illumination, however, regardless of the presence of organic compounds, the anodic photocurrent increased initially with potential bias then reached saturation. Irrespective of the chemical identities, voltammograms obtained from all organic compounds investigated revealed similar photocurrent/potential (I/E) characteristics to those shown in Fig. 1.

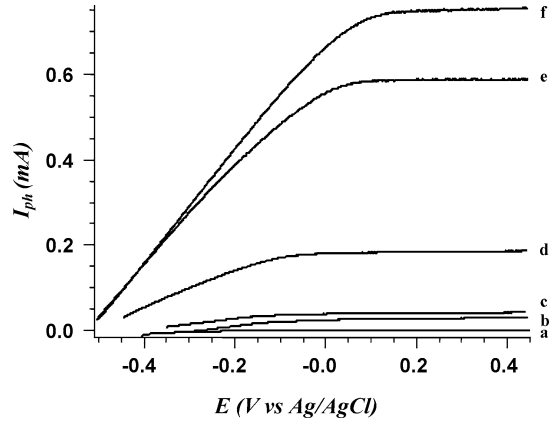

Fig. 1. The typical voltammograms of oxalic acid at TiO_2 porous electrodes with and without UV illumination in 0.1 M $NaNO_3$ containing different concentrations of oxalic acid at pH 4.0: (a) in the presence and the absence of oxalic acid in the dark, (b) in the absence of oxalic acid under illumination, (c) 0.1 mM oxalic acid, (d) 2 mM oxalic acid, (e) 7 mM oxalic acid, (f) 10 mM oxalic acid.

As previously reported [16,25], the overall photocatalytic process is controlled by photoelectron transport across the semiconductor film in the linear part of the I/E curve and by the overall interfacial reaction in the saturated part of the I/E curve. As such, a potential bias of $+0.30$ V was selected for all subsequent photoelectrolysis experiments because the measured data at this potential are indicative of the kinetics of the interfacial process and are not affected by the removal and transport of electrons across the film. In addition, the direct electrochemical oxidation/reduction of water at bare ITO sites does not occur at this potential. Hence, the background photocurrent resulting from the photooxidation of water is essentially constant and could be accurately deducted.

3.2. Measurement of adsorption by transient photoelectrolysis

Initially the TiO_2 porous film electrode was immersed in a solution containing the organic compound to allow adsorption of the organic. Once adsorption equilibrium was reached, the electrode was removed from the adsorption solution and carefully washed before it was transferred into a blank electrolyte solution to perform the photoelectrolysis measurement. The amount of adsorption (or surface coverage of the electrode) is governed by the experimental conditions and the thermodynamics of the adsorption system, which can be quantified through an exhaustive photoelectrolysis process as previously reported [15]. According to this measurement principle, the net charge obtained from the

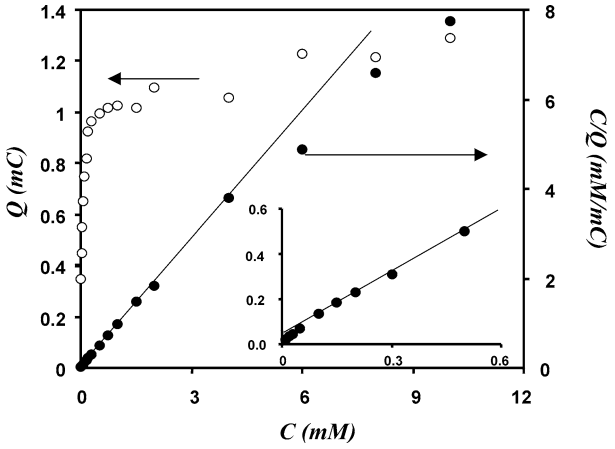

Fig. 2. The adsorption isotherm of oxalic acid preadsorbed at pH 4.0 and the resultant data treatment according to Langmuir adsorption model. The insert is the resultant data at low concentrations.

exhaustive photoelectrolysis of the adsorbed organic compound is directly proportional to the amount of adsorption or surface coverage. Therefore, the adsorption isotherm of the adsorbate can be obtained by plotting the net charge obtained from electrodes (equilibrated in various concentrations of adsorbate) against the corresponding adsorption solution concentration [15].

Fig. 2 shows the adsorption isotherm of oxalic acid and the resultant data treatment according to the Langmuir adsorption model [22]. The experimental data revealed that the Langmuir adsorption model was well followed in the medium concentration range. Deviation from the Langmuir adsorption model in very low and high concentration regions was observed, indicative of different adsorption behaviour at different concentrations. These differences in adsorption behaviour may be attributed to the formation of different types of surface complexes. Three different types of adsorption characteristics indicate that there are at least three different types of surface complexes and each has a different binding strength to the TiO_2 surface. Hug and Sulzberger [26] also reported a similar finding during their study of oxalic acid adsorption at the TiO_2 surface with an in situ FTIR spectroscopic technique. They obtained three different surface complexes each having a distinct adsorption equilibrium constant. They believe this was caused by the heterogeneity of the TiO_2 surface.

The strongest bound complex is formed at very low concentrations and the corresponding charge obtained indicates that this type of complex accounts for a very small fraction of the total adsorbed amount. According to Regazzoni et al. [13], surface titanium ions at the crystal edges and corners, with fewer coordination positions occupied by O^{2-}, display the highest affinity for adsorbing ligands and the number of these ions is limited. The strongest surface-bound complex can be attributed to adsorption at such sites. The medium-strength surface-bound complex is responsible for the Langmuir behaviour in the medium concentration range and this type of complex accounts for the vast majority of the total adsorption as demonstrated by the corresponding charge measured. The weakest bound complex formed at high concentrations accounts for a small portion of the total adsorption quantity. Titanium ions from the most stable, perfectly cleaved (001) and (011) crystal faces of anatase, which are penta-coordinated to O^{2-} ions and complete their coordination sphere by binding OH^-, are responsible for the latter two types of surface complexes. The overall adsorption characteristics of oxalic acid is similar to previously reported adsorption of salicylic acid on TiO_2 surfaces [13]. Interestingly, similar results were obtained from the adsorption of other dicarboxylic acids such as malonic acid, succinic acid, and glutaric acid. This suggests that different dicarboxylic acids possess similar adsorption behaviour.

3.3. Kinetics of photoelectrolysis of adsorbed oxalic acid

Theoretically, it is widely recognised that a heterogeneous photocatalytic reaction should be a first-order reaction with respect to both the surface coverage of organic adsorbates and the photohole concentration at the surface [27]. In practice, however, the experimental data often deviate from a first-order reaction with respect to the surface coverage. This has been reported to be the result of the heterogeneity of the photocatalytic surface [28]. If a uniform catalytic surface is covered by only one type of species, then a first-order rate law with surface coverage should always be applicable. However, more than one type of surface complex may be formed when a heterogeneous catalytic surface is in contact with a single species in solution. Under this circumstance, the overall catalytic process is the result of contributions by the individual catalytic process of each type of surface complex, and the normal first-order rate law with respect to surface coverage cannot be used to represent the overall catalytic processes. Nevertheless, the normal first-order rate law should still be applicable to the individual catalytic processes of each type of surface-bound complex.

As demonstrated in Fig. 2, the overall adsorption isotherm for oxalic acid at the TiO_2 electrode is potentially the result of three different types of surface complexes. If this were the case, the photocurrent decay curves may not follow a simple, single exponential decay. This was indeed the case for the photocurrent decay curves recorded for the photocatalytic breakdown of adsorbed oxalic acid at these electrodes. Furthermore, the photocurrent decay curves revealed that the apparent half-life of these oxidation processes varied with surface coverage (or the amount adsorbed). This indicates that such a catalytic process cannot be represented by simple first-order kinetics. We believe it is possible to study the kinetics at heterogeneous catalytic surfaces if we can identify the individual contributions to the overall catalytic process.

If we assume that the overall photocatalytic process is the sum of the individual photocatalytic processes of each type of surface complex, then the total photocurrent, I_{ph}, can be

described as

$$I_{ph} = \sum_{j=1}^{n} I_{phj}, \tag{1}$$

where I_{ph} refers to the total instantaneous photocurrent; I_{phj} is the instantaneous photocurrent generated from photocatalytic oxidation of j type of surface complexes.

If we also assume that a normal first-order rate law with respect to surface coverage can be applied to represent the individual catalytic processes of each type of surface complex, then the rate of reaction for a particular surface complex can be given as

$$Rate_j = -\frac{\mathrm{d}\theta_j}{\mathrm{d}t} = \frac{I_{phj}}{nF} = k\theta_j[h^+]_s, \tag{2}$$

where θ_j is the surface coverage of the j type of surface complex and is defined by the ratio of surface concentration of this species, C_{sj}, to the saturated surface concentration, C_{ssj} (i.e., C_{sj}/C_{ssj}); n is the number of electrons transferred during the photocatalytic mineralization of j species and F is the Faraday constant; $[h^+]_s$ is the surface concentration of photoholes at this type of site.

When a suitable potential bias is applied, for a given electrode and light intensity, C_{ssj} and $[h^+]_s$ are constants. Equation (2) can therefore be rewritten as

$$Rate_j = -\frac{\mathrm{d}C_{sj}}{\mathrm{d}t} = \frac{I_{phj}}{nF} = k_j C_{sj}. \tag{3}$$

At $t = 0$, the initial photocurrent I^0_{phj} is determined by the initial surface concentration of the adsorbed j species:

$$I^0_{phj} = nFk_j C^0_{sj}. \tag{4}$$

Solving the differential Eq. (3) and consideration of Eq. (4) gives

$$\begin{aligned} I_{phj} &= I^0_{phj}\exp(-k_j t) = nFk_j C^0_{sj}\exp(-k_j t) \\ &= k_j Q^0_j \exp(-k_j t), \end{aligned} \tag{5}$$

where Q^0_j is the charge expected for the mineralization of j adsorbed species.

Substitution of Eq. (5) into Eq. (1) gives

$$\begin{aligned} I_{ph} &= \sum_{j=1}^{n} I^0_{phj}\exp(-k_j t) = \sum_{j=1}^{n} nFk_j C^0_{sj}\exp(-k_j t) \\ &= \sum_{j=1}^{n} k_j Q^0_j \exp(-k_j t). \end{aligned} \tag{6}$$

Equation (6) indicates that the total photocurrent decay profile can be represented by the sum of individual exponential components corresponding to the degradation of each type of adsorbed surface complex. From this kinetic model, information on both the adsorption amount of each adsorbed species and their photocatalytic reactivity can be obtained.

Fig. 3 shows the photocurrent decay curves for the photocatalytic oxidation of oxalic acid adsorbed onto TiO_2 from two different solution concentrations (0.05 and 8.0 mM). In both cases, it was shown that the photocurrent decay profiles of the adsorbed oxalic acid could be well curve-fitted to a double exponential expression (NB: attempts to curve fit to a single exponential expression were unsuccessful). At other surface coverages, the decay curves were equally well fitted to a double exponential expression. That is,

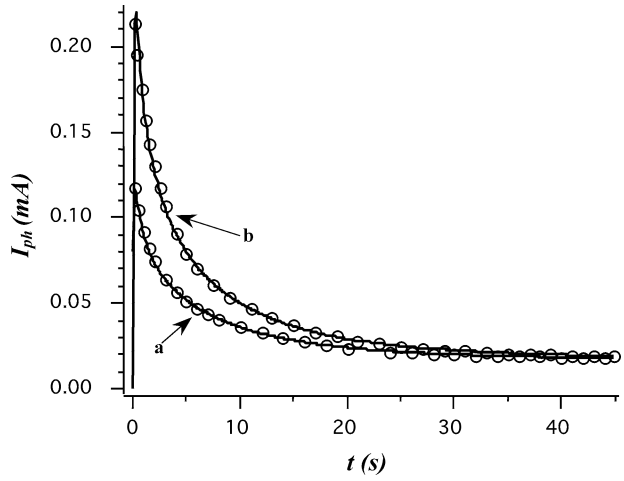

Fig. 3. The photocurrent decay curves for the photocatalytic oxidation of oxalic acid adsorbed onto TiO_2 from two different solution concentrations at pH 4.0, 0.05 mM (a), and 8 mM (b), and the curve-fitting data (○).

$$I_{ph} = a_0 + a_1\exp(-a_2 t) + a_3\exp(-a_4 t), \tag{7}$$

where I_{ph} referred to the total photocurrent; a_0, a_1, a_2, a_3, and a_4 are constants and t is the time lapsed from the onset of illumination.

Of the constants in Eq. (7) only a_0 is independent of the chemical nature and the surface coverage of a specific species, and can be attributed to the steady-state oxidation photocurrent of water, which is irrelevant to the oxidation of adsorbed organic compounds. The double exponential decay of photocurrent implies there are two decay processes with different half-lifes. This kind of double exponential response suggests that two distinct photocatalytic processes with different degradation rates occurred simultaneously at the same electrode surface. Although there may be three different types of surface complexes identified from the adsorption study, kinetically, only two distinct decay processes were found, which indicates that one species has quite a different photocatalytic reactivity from the other two species. The two distinct kinetic processes represent two kinetically different adsorbed species—one is fast (denoted as f) and another is slow (denoted as s). That is, for photocatalysis of adsorbed oxalic acid, Eq. (6) can be rewritten as

$$\begin{aligned} I_{ph} &= I^0_{phf}\exp(-k_f t) + I^0_{phs}\exp(-k_s t) + k_w \\ &= k_f Q^0_f \exp(-k_f t) + k_s Q^0_s \exp(-k_s t) + k_w, \end{aligned} \tag{8}$$

where k_s and k_f represent the rate constant for the fast and slow kinetic processes, respectively, and are independent of the amount adsorbed; Q^0_f and Q^0_s are the charge generated

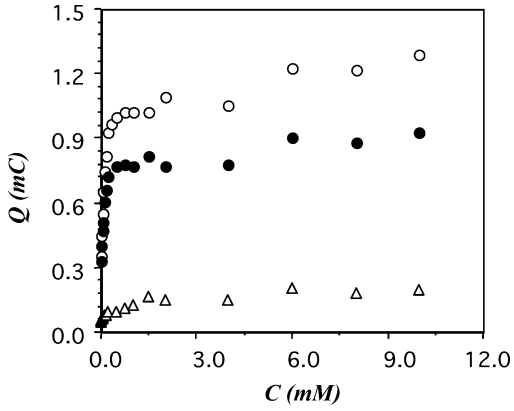

Fig. 4. The adsorption isotherms of the fast and slow kinetic components, and the total for oxalic acid: (○) total adsorption, (●) adsorbed species responsible for the slow kinetic process, (△) adsorbed species responsible for the fast kinetic process.

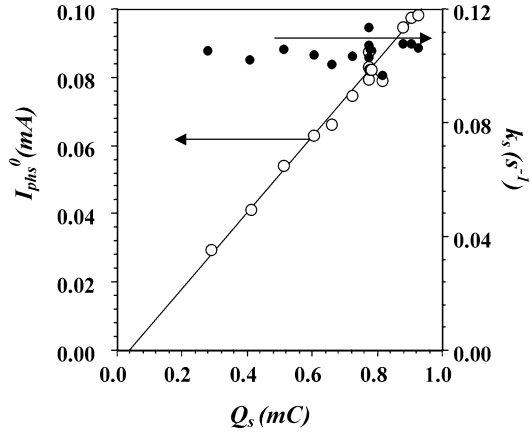

Fig. 5. A plot of I_{phs}^0 and k_s versus the amount adsorbed (oxalic acid) (Q_s) for the slow kinetic species: (○) first-order constant (k_s), (●) initial reaction rate (I_{phs}^0).

from the mineralization of the surface bound species responsible for the fast and slow processes, respectively.

Comparisons of Eqs. (7) and (8) give the following relationships:

$$I_{phf}^0 = a_1, \quad k_f = a_2, \quad I_{phs}^0 = a_3,$$
$$k_s = a_4, \quad \text{and} \quad k_w = a_0.$$

The charge generated from the mineralization of the surface-bound species responsible for the fast and slow processes can be expressed as

$$Q_f^0 = a_1/a_2, \quad Q_s^0 = a_3/a_4.$$

It is important to note that Q_f^0 and Q_s^0 represent the initial adsorbed amounts (or the surface coverage) of the surface-bound species responsible for the fast and slow processes, respectively. The above discussion suggests that kinetic parameters such as I_{phf}^0, I_{phs}^0, Q_f^0, Q_s^0, k_f, k_s, and k_w can be obtained by comparing the empirical kinetic model (Eq. (7)) with the theoretical kinetic model (Eq. (8)).

Using this approach, it was possible to deconvolute the total adsorption isotherm in Fig. 2, into its fast and slow kinetic components. These data are shown in Fig. 4, where it can be seen that the amount of surface-bound species responsible for the slow process exhibited a similar trend to the total adsorption isotherm (see Fig. 2) and accounts for most of the adsorption quantity, particularly, at higher solution concentrations. The slow kinetic process can be attributed to the photocatalytic degradation of the intermediate and weakly bound surface complexes. It was also found that the amount of surface-bound species responsible for the fast process can be easily saturated at low concentrations and accounted for only a small portion of the total adsorption quantity. This species can be identified as the strongest bound surface complex.

Equation (8) predicts that I_{phs}^0 and I_{phf}^0 should be directly proportional to Q_s^0 and Q_f^0, respectively, while k_s and k_f are independent of Q_s^0 and Q_f^0, respectively. Both I_{phs}^0

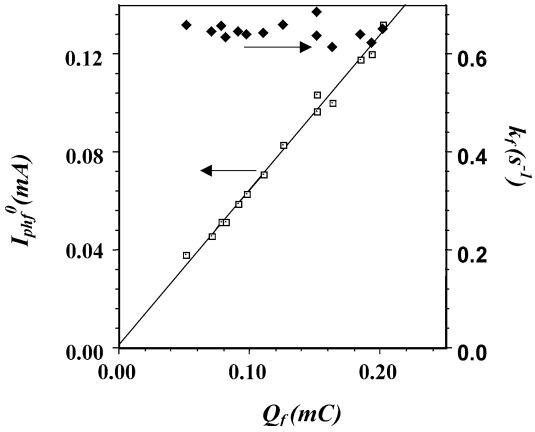

Fig. 6. A plot of I_{phf}^0 and k_f versus the amount adsorbed (oxalic acid) (Q_f) for the fast kinetic species, (◆) first order rate constant (k_f), (⊡) initial reaction rate (I_{phf}^0).

and I_{phf}^0 can be obtained from the constants of the curve-fitted photocurrent decay curves (i.e., a_3 and a_1). Similarly, k_s and k_f can also be obtained from this data (i.e., a_4 and a_2).

A plot of I_{phs}^0 and k_s versus the amount adsorbed (Q_s) for the slow kinetic species is shown in Fig. 5. As predicted by Eq. (8), it was found that the initial photocurrent (or initial rate) associated with the slow kinetic process (I_{phs}^0) was proportional to the initial surface coverage of the species responsible for the slow process (i.e., the intermediate and weakest bound complexes). It was also shown that the first-order rate constant associated with the slow process remained almost unchanged with the initial surface coverage. This was also predicted by Eq. (8). The average value of k_s over the entire range of surface coverage was found to be ca. 0.10 s^{-1}.

A plot of I_{phf}^0 and k_f versus the amount adsorbed (Q_f) for the fast kinetic species is shown in Fig. 6. Again, it was found that the initial photocurrent or reaction rate was directly proportional to the amount of the adsorbed species

(i.e., the strongest bound complex) and the rate constant (k_f) was independent of the adsorption amount. The average value of the rate constant for the fast kinetic species over the entire range of the surface coverage was found to be ca. 0.61 s^{-1}, which is approximately 6 times faster than the slow kinetic process.

The photocatalytic oxidation of the adsorbed species responsible for both the fast and the slow kinetic processes complies well with the first-order reaction kinetics. This multisite adsorption model explains the photocatalytic oxidation of adsorbed oxalic acid very well.

3.4. Extension of the kinetic model to more complicated adsorbates

The approach described above was subsequently employed to study the kinetics of photoelectrolysis of larger dicarboxylic acids that, compared to oxalic acid, ought to undergo more degradative steps and involve more intermediates during their mineralization. This was done to elucidate what influence the breakdown intermediates have on the overall photocatalytic degradation kinetics. It was found that at low adsorption concentration (or surface coverage), the photocurrent decay profiles of all dicarboxylic acids investigated were similar to those of oxalic acid and the transient photocurrent responses could be fitted to the double exponential expression described above. However, at higher surface coverage, the results from the double exponential curve fitting showed that the value of the constant (a_2) associated with the fast process approached the value of the constant (a_4) associated with the slow process. In other words, the photocurrent decay curve approached a single exponential decay representing the slow process only. As the surface coverage was further increased it was found that the initial part of the photocurrent decay curves could not be fitted to any exponential decay, while the remainder of the photocurrent decay curve could still be fitted to a single exponential decay.

Fig. 7 shows the photocurrent decay profiles and the curve-fitting data for adsorbed glutaric acid at different surface coverages. At low surface coverage, the decay curve (a) can be fitted to a double exponential expression. At medium surface coverage, the decay curve (b) approaches a single exponential decay. At high surface coverage, the initial part of decay curve (c) is deformed to the point that it cannot be fitted to any exponential decay, while the remainder of curve (c) follows a single exponential decay. This shift from double exponential decay (representing fast and slow processes) to a single exponential decay with increasing surface coverage was observed for all the larger dicarboxylic acids. A related study (unpublished data) showed that this was also the case for a wide range of aromatic compounds, which, like the larger dicarboxylic acids, involve a series of degradative steps and intermediate breakdown products.

Fig. 8 shows a plot of rate constants for the fast process (k_f) (calculated form the curve-fitting data) versus surface coverage (Q_f) for the different dicarboxylic acids. For all of the larger dicarboxylic acids the rate constants were found to decrease with surface coverage, whereas the k_f values for oxalic acid remained constant (as shown previously in Fig. 5). Interestingly, although the k_f values change with surface coverage (indicating that the fast process does not follow first-order kinetics) the trend with respect to surface coverage was very similar for all the larger dicarboxylic acids. This suggests that the overall rate characteristics of the larger dicarboxylic acids (i.e., excluding oxalic acid) are not overly influenced by their specific chemical structures. Rather, the similar rate characteristics (for the larger dicarboxylic acids) are due to the fact that the same amounts of charge (the amount adsorbed) for different dicarboxylic acids should have same equivalent adsorbate concentrations or same total "photohole demand" (NB: "photohole demand" refers to the number of photoholes needed for

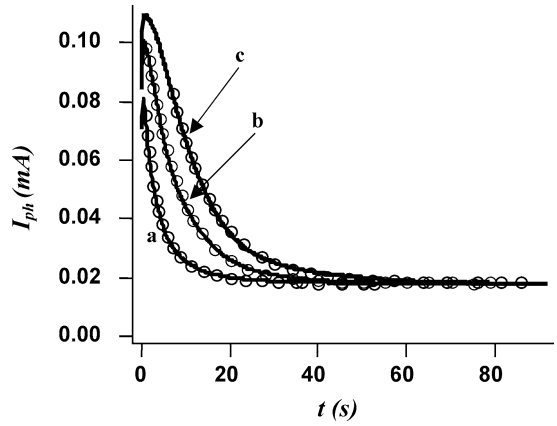

Fig. 7. The photocurrent decay profiles (solid lines) and the curve-fitting data (circles) for glutaric acid preadsorbed in 0.1 M $NaNO_3$ with different glutaric acid concentrations at pH 4.0, 0.04 mM (a), 0.5 mM (b), and 5 mM (c). Solid black lines are the experimental curves.

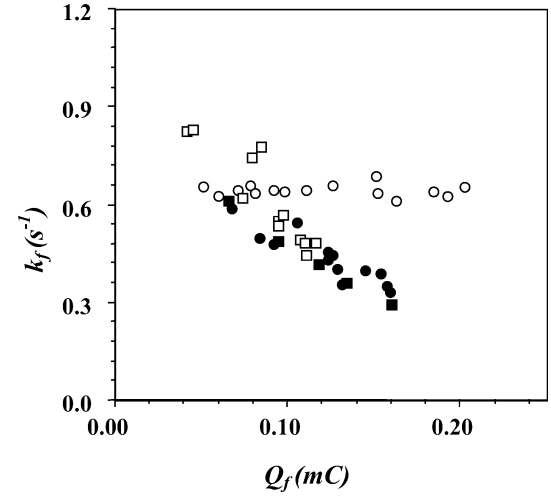

Fig. 8. A plot of rate constants for the fast kinetic process (k_f) (calculated form the curve-fitting data) versus surface coverage (Q_f) for the different dicarboxylic acids preadsorbed from different concentrations of acids at pH 4.0, (○) oxalic acid, (●) malonic acid, (□) succinic acid, (■) glutaric acid.

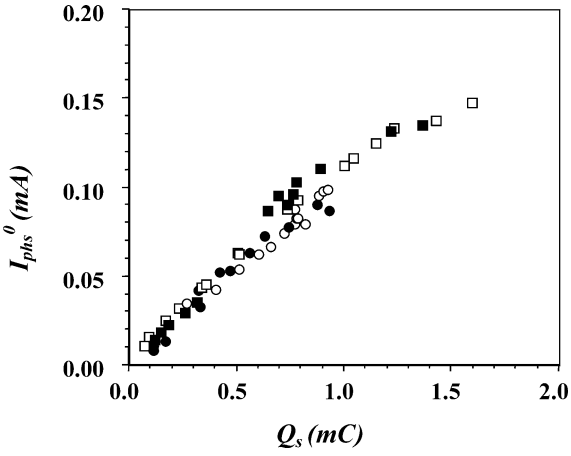

Fig. 9. A plot of I_{phs}^{0} values versus Q_s values for the dicarboxylic acids preadsorbed from different concentrations of acids at pH 4.0: (○) oxalic acid, (●) malonic acid, (□) succinic acid, (■) glutaric acid.

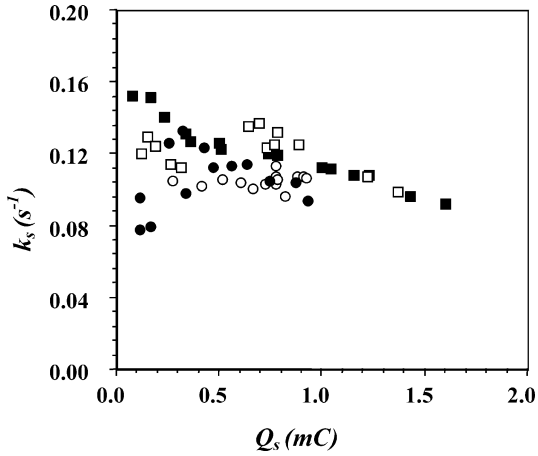

Fig. 10. The plot of k_s versus Q_s for all the dicarboxylic acids preadsorbed from different concentrations of acids at pH 4.0: (○) oxalic acid, (●) malonic acid, (□) succinic acid, (■) glutaric acid.

the breakdown of the organic molecule), but have different numbers of adsorbed molecules. Given that different dicarboxylic acids have similar adsorption behaviour and the main difference between the larger dicarboxylic acids and oxalic acid lies in the number of degradative steps and intermediates formed during photocatalytic mineralization, the differences in the photocurrent responses are most likely caused by accumulation of intermediates at the electrode surface. Compounding the problem is the fact that there are more complex photohole demand characteristics for the larger dicarboxylic acids compared with the relatively simple (two) photohole demand for oxalic acid, causing less even distribution of total photohole demand over the electrode surface. This may actually lead to a higher photohole/photoelectron recombination rate as adsorbed intermediates can act as photohole/photoelectron recombination centers. This latter argument is further justified by the fact that at higher light intensities (and therefore higher photohole concentrations) the fast kinetic process for the larger dicarboxylic acids is less influenced by surface coverage—thus bringing it closer to the oxalic acid case.

Examination of the slow kinetic process was also carried out for the larger dicarboxylic acids. Fig. 9 shows a plot of I_{phs}^{0} values versus Q_s values for the dicarboxylic acids. As in Fig. 6 [and predicted by Eq. (8)] a linear relationship was observed between I_{phs}^{0} and Q_s. Importantly, the slopes of these relationships were the same for all of the dicarboxylic acids (including oxalic acid). This indicated that, for the slow process (associated with destruction of the intermediate and weakly bound surface complexes), there appears to be no discernible differences in the photocatalytic responses due to the differing chemical nature of each adsorbate. In other words the photohole concentration (at this light intensity) was sufficient to keep up with the photohole demand of the slow process for all adsorbates.

This assertion was further supported by the data in Fig. 10, which shows the plot of k_s versus Q_s for all the dicarboxylic acids. The data indicate that the reaction rate constant for the slow process (k_s) remained essentially constant with increasing surface coverage (Q_s). At low surface coverage values, there is a noticeable spread of k_s values for the different adsorbates. This was probably due to the error involved in measuring (and curve fitting) the photoelectrochemical responses from the small amounts of adsorbed species (relative to the H_2O background). At higher surface coverage values, the k_s values became more constant (i.e., $\sim 0.10\ s^{-1}$) and seem to be independent of the chemical nature of the dicarboxylic acid.

In a general sense, the overall photocatalytic response for the breakdown of adsorbed dicarboxylic acids seems to be due to a fast kinetic component and a slow kinetic component. The slow process (associated with intermediate and weakly bound surface complexes) seems not to be affected by the chemical identity/nature of the dicarboxylic acid. On the other hand, the fast process, associated with strongly bound surfaces complexes, was shown to be markedly different for the simple dicarboxylic acid (i.e., oxalic acid) compared to the larger compounds. This was due to the different photohole demand characteristics of the different compounds and the fact that the concentration of photoholes (at the light intensity used) was not sufficient to quickly and fully degrade the larger compounds (and corresponding intermediates) when compared to the smaller/simpler oxalic acid.

4. Conclusion

A transient photoelectrolysis technique has been developed, by which the photocatalytic oxidation of adsorbed organic compounds can been studied from a different perspective. The photocatalytic oxidation of adsorbed oxalic acid complies well with a multisite or multimode kinetic model. While three types of thermodynamic surface-bound complexes were evident, only two types of kinetic processes were identified—a fast and a slow process. Each process

was shown to follow first-order reaction kinetics. The fast kinetic process is due to the photocatalytic degradation of the strongest surface-bound complex, accounting for a small portion of the total amount adsorbed. The slow kinetic process is due to the photocatalytic degradation of the medium and the weakest surface-bound complexes, accounting for most of the total amount of adsorption.

For the photocatalytic oxidation of larger dicarboxylic acids adsorbed, the fast process was found not to follow first-order reaction kinetics. The rate decreased as the surface coverage increased. This may be attributed to a longer dwelling time of such adsorbates (or intermediates) at the electrode surface due to a larger photohole demand and less even distribution of the demand at the electrode surface compared to oxalic acid. The slow process, however, was found to follow first-order reaction kinetics.

Acknowledgment

The financial support by ARC (Australian Research Council) is greatly acknowledged.

References

[1] P. Mandelbaum, A.E. Regazzoni, M.A. Blesa, S.A. Bilmes, J. Phys. Chem. B 103 (1999) 5505.
[2] S. Yamazaki, S. Tanaka, H. Tsukamoto, J. Photochem. Photobiol. A: Chem. 121 (1999) 55.
[3] H. Al-Ekabi, N. Serpone, E. Pelizzetti, C. Minero, M.A. Fox, R.B. Draper, Langmuir 5 (1989) 250.
[4] J. Cunningham, G. Al-Sayyed, J. Chem. Soc., Faraday Trans. 86 (1990) 3935.
[5] B. Jenny, P. Pichat, Langmuir 7 (1991) 947.
[6] T.A. Heimer, E.J. Heilweil, C.A. Bignozzi, G.J. Meyer, J. Phys. Chem. B 104 (2000) 4256.
[7] F. Zhang, J. Zhao, T. Shen, H. Hidaka, E. Pelizzetti, N. Serpone, Appl. Catal. B: Environ. 15 (1998) 147.
[8] C. Kormann, D.W. Bahnemann, M.R. Hoffmann, Environ. Sci. Technol. 25 (1991) 494.
[9] M.R. Hoffmann, S.T. Martin, W. Choi, D.W. Bahnemann, Chem. Rev. 95 (1995) 69.
[10] N. Serpone, E. Pelizzetti, Photocatalysis, Fundamentals and Applications, Wiley, New York, 1989.
[11] Y. Xu, C.H. Langford, Langmuir 17 (2001) 897.
[12] Y. Xu, C.H. Langford, J. Photochem. Photobiol. A: Chem. 133 (2000) 67.
[13] A.E. Regazzoni, P. Mandelbaum, M. Matsuyoshi, S. Schiller, S.A. Bilmes, M.A. Blesa, Langmuir 14 (1998) 868.
[14] S. Kim, W. Choi, Environ. Sci. Technol. 36 (2002) 2019.
[15] D. Jiang, H. Zhao, S. Zhang, R. John, G.D. Will, J. Photochem. Photobiol. A: Chem. 156 (2003) 201.
[16] D. Jiang, H. Zhao, S. Zhang, R. John, J. Phys. Chem. B, in press.
[17] H.Y. Chen, O. Zahraa, M. Bouchy, F. Thomas, J.Y. Bottero, J. Photochem. Photobiol. A: Chem. 85 (1995) 179.
[18] A. Hagfeld, M. Gratzel, Chem. Rev. 95 (1995) 49.
[19] J. Cunningham, P. Sedlak, J. Photochem. Photobiol. A: Chem. 77 (1994) 255.
[20] B. Ohtani, S.-i. Nishimoto, J. Phys. Chem. B 97 (1993) 920.
[21] S. Tunesi, M. Anderson, J. Phys. Chem. B 95 (1991) 3399.
[22] G.N. Ekstrom, A.J. McQuillan, J. Phys. Chem. B 103 (1999) 10562.
[23] A.D. Roddick-Lanzilotta, A.J. McQuillan, J. Colloid Interface Sci. 227 (2000) 48.
[24] M.K. Nazeeruddin, A. Kay, I. Rodicio, R. Humphry-Baker, E. Muller, P. Liska, N. Vlachopoulos, M. Gratzel, J. Am. Chem. Soc. 115 (1993) 6382.
[25] D. Jiang, H. Zhao, Z. Jia, J. Cao, R. John, J. Photochem. Photobiol. A: Chem. 144 (2001) 197.
[26] S.J. Hug, B. Sulzberger, Langmuir 10 (1994) 3587.
[27] S.R. Morrison, Electrochemistry at Semiconductor and Oxidized Metal Electrodes, Plenum, New York, 1980.
[28] W.J. Albery, P.N. Bartlett, C.P. Wilde, J.R. Darwent, J. Am. Chem. Soc. 107 (1985) 1854.